5340

UNCLASSIFIED

NRL Report 7050

Simulated Ocean Radar Impulse Responses From Lunar Radar Measurements

A. SHAPIRO, B. S. YAPLEE, AND E. A. ULIANA

E. O. Hulburt Center for Space Research
Space Science Division

May 7, 1970

NAVAL RESEARCH LABORATORY
Washington, D.C.

This document has been approved for public release and sale; its distribution is unlimited.

CONTENTS

UNCLASSIFIED

ABSTRACT

Measurements of the radar impulse response from rough surfaces should provide criteria for relating the radar return with the vertical structure of these surfaces. Such information is needed to utilize more efficiently ocean satellite radar observations for describing sea surface structure. While no direct measurements of the radar impulse response are available from a fluid surface, the NRL lunar high-range-resolution radar observations can provide equivalent radar impulse response measurements from a solid rough surface. The lunar radar measurements were used to simulate the ocean impulse response, and thus provide some insight into the effect of different surface roughnesses on the radar return.

The radar returns from five lunar areas of different surface roughness were analyzed and the impulse response derived. The results indicate that the size of the vertical structure correlates with the width of the impulse response, and that quantitative information concerning the parameters of mean height and surface roughness can be obtained by computing the power centroid and standard deviation of the impulse response. However, due to the nonuniform distribution of the lunar surface features, the two parameters will depend on the particular location of the surface features and the scanning speed of the radar observations.

The geometry of the ocean satellite radar observations is similar to that of the lunar radar observations, and because of the more uniform distribution of the vertical surface structure of a fluid surface, it can be expected that ocean impulse response measurements would provide more consistent data on the mean height and associated water wave heights of the observed water surface.

PROBLEM STATUS

This is an interim report on a continuing problem.

AUTHORIZATION

NRL Problem G01-05
Project A37-538/F48-551-702

Manuscript submitted January 7, 1970.

UNCLASSIFIED

SIMULATED OCEAN RADAR IMPULSE RESPONSES FROM LUNAR RADAR MEASUREMENTS

INTRODUCTION

The measurement of the radar impulse response of the ocean surface for different sea states would provide a description of both the large-scale and small-scale electromagnetic reflection properties of the sea surface. If a relation can be established between the radar impulse response and the geometric distribution of the sea surface, it will then be possible to obtain information about the sea surface structure from radar observations. As one step in this direction, the impulse response of solid surfaces, which have much larger vertical structure, could be measured and used to obtain a better understanding of the reflection properties and the nature of complex surfaces in general. Previous measurements of this latter type were available at NRL, and an analysis of the data could provide guidelines, after proper scaling, for producing an equivalent ocean impulse response.

A radar system can be defined as a device that measures the impulse response of space. This definition implies that the basic function of a radar is the determination of the volume distribution of reflecting matter in a finite column, and that this can be achieved by probing a cylindrical volume with an impulse of high spatial resolution. This concept, if applied to radar observations of rough surfaces at normal incidence, would provide a graphic description of the vertical surface structure distribution, in terms of the surface reflecting properties. In practice, measurements of the impulse response can only be approximated since the constraints of the radar performance and the geometry of the observations restrict the full implementation of the desired measurement process. The measurements would require a very large bandwidth and large antenna sizes if the observations are to be restricted to narrow cylindrical volumes. However, if a uniform surface structure can be assumed, then radar observations made with limited antenna sizes operating under pulse-width-limited conditions can be processed to obtain an equivalent impulse response. This assumption should be valid for a fluid surface, such as the ocean. The same data processing, if applied to radar observations of solid surfaces, will be more difficult to interpret since, in general, the surface structure may not be uniformly distributed and the locations of the specific reflecting features may not be known. However, a more uniform surface structure can be at least partially simulated if the observing platform scans across the surface so that specific surface features will be moved into different radar range intervals during the integration period of the radar returns.

The NRL high-range-resolution lunar radar data, which were obtained under pulse-width-limited conditions, will be utilized to show the effect of different vertical surface structures on the shape of the radar returns, and the equivalent mean height and size of the vertical large-scale surface structure will be derived. The results will be evaluated in terms of their internal consistency and physical significance. This report will conclude with a discussion of the application of the results to radar observations of the ocean from a space platform.

GEOMETRIC CONSTRAINTS OF THE LUNAR RADAR OBSERVATIONS

The NRL lunar radar observations measured the radar return from different areas in the central region of the moon, as shown in Fig. 1. During the period of observations the locus of the subearth point described approximately an ellipse over a one-month period of time due to lunar librations, and for a given day the path for the motion of the subearth point was a short line segment. In the discussion, five areas are selected which cover the range of topographic variations that were encountered in the Sinus Medii region. They are, in order of increasing roughness, the areas near the craters Hyginus, Mösting, Ukert, Lalande, and Herschel.

The effective transmitted pulse width τ was about 1 μs and the observations were performed under the pulse-width-limited conditions shown in Fig. 2. It is seen from the geometry that the radar energy would be returned sequentially from a series of concentric annular rings if the vertical dimension of the surface structure of a rough surface is

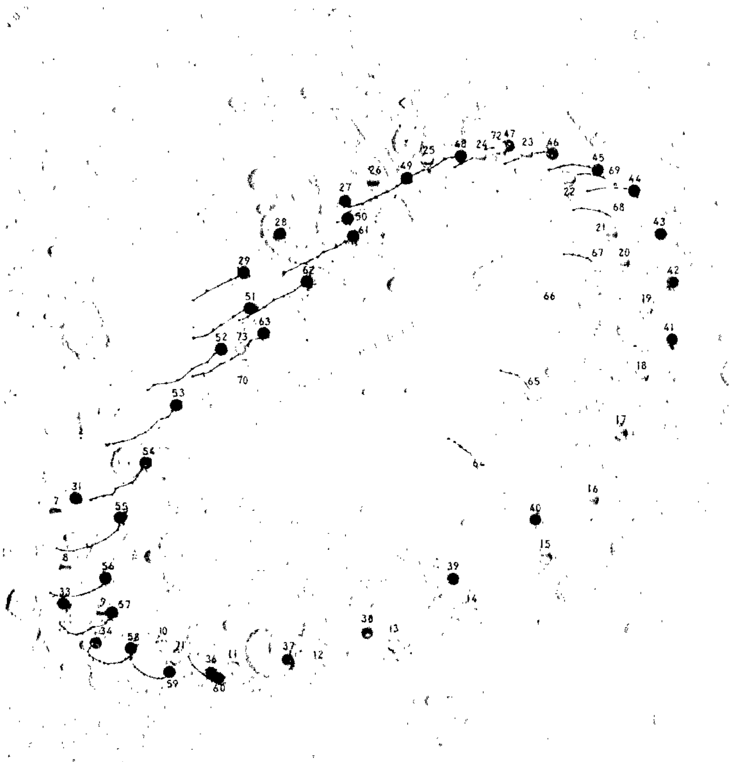

Fig. 1 - Sinus Medii region of the moon from which radar data had previously been collected by NRL. This data was used to study the effect of different vertical surface structures on the shape of radar returns (echoes), and then to derive the equivalent mean height and size of these structures. The short line segments describe the motion of the subearth point over one-day periods of observation.

UNCLASSIFIED

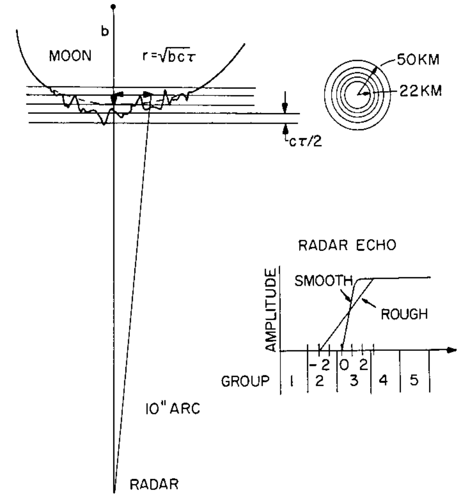

Fig. 2 - Simplified geometry associated with lunar radar echoes under pulse-width-limited conditions. In the relation $r = \sqrt{bc\tau}$, r is the horizontal range resolution, at the lunar surface, determined by the characteristics of the radar pulse, b is the lunar radius, τ is the width of the pulse, and c is the speed of light.

less than the range resolution. The effect of a large vertically extended surface structure is also shown in Fig. 2, where the height associated with such a surface feature is, in this case, spread over five range resolution intervals. For a uniform roughness and surface distribution the rise time of the radar echo will increase to five range resolution intervals. When the full amplitude of the echo is reached, the received power will be proportional to the scattered power contained in five contiguous annular rings, with the reflection being characteristic of the different height layers in each ring. Thus if one is concerned primarily with the power reflected from the initial circular area, it is necessary to obtain the power difference between the adjacent range resolution intervals, which for uniform reflection characteristics and small angles of incidence will then provide an estimate of the impulse response of the initial area. The power in each range resolution interval is then proportional to the average reflected power from two adjacent annular rings.

The assumption of uniform surface structure, while valid for the ocean surface, will not apply to the lunar surface since high lunar mountains may be located near large smooth surfaces, giving a nonsymmetrical distribution within the relatively small observation volume. Thus, while the impulse response of the lunar echo may not correspond to the initial area as desired, it can be considered as a pseudoimpulse response of a larger area, and thus provide a signature of the observation volume. If one averages the many returns of a radar which scans the surface so that the different surface features are shifted into different annular rings, a more uniform surface structure will be simulated. This means that for a solid surface the spatial resolution is degraded by the surface structure, and the energy may be due to either a low area in the initial volume or a high plateau located in the later annular rings. In some simple cases (Fig. 3) the ambiguity of location can be resolved by an analysis of the time history of the radar echo as the radar scans across the surface.

LUNAR RADAR DATA

In Fig. 4 individual radar echoes from a relatively smooth area (Hyginus) are shown. Even though a high signal-to-noise ratio is available, the rapid fluctuations of the amplitude makes it difficult to obtain any accurate information about the corresponding surface structure. The variations in amplitude are due to phase interference of many small reflecting facets similar to that obtained from sea clutter. After 300 of these echoes are

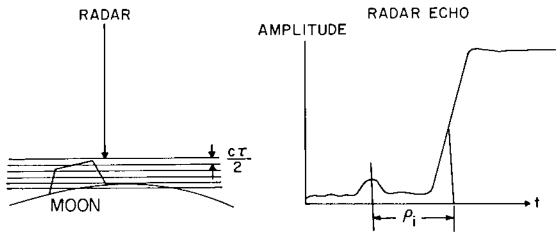

Fig. 3 - Characteristic lunar radar echo of a low area bordered by a high plateau. When there is relative transverse motion between the radar and the object being scanned, as there is with the moon, the unambiguous location of surface features can be determined only in simple cases, such as the one illustrated.

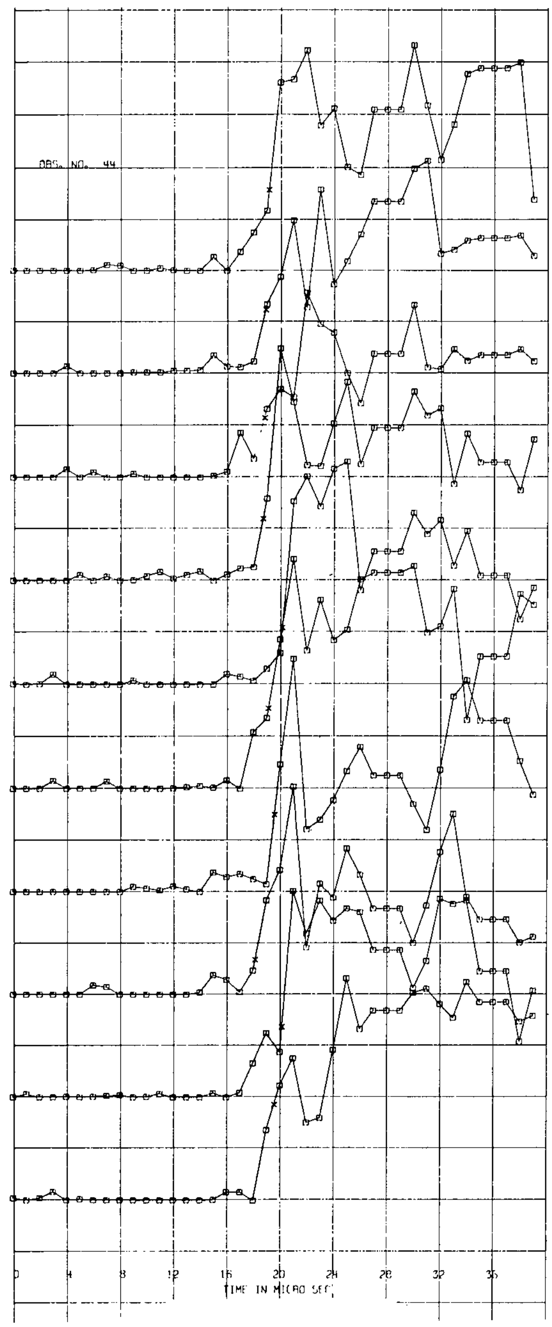

Fig. 4 - Individual radar echoes of the relatively smooth Hyginus area of the moon. The echoes were obtained at 9-s intervals.

UNCLASSIFIED

averaged, a more regular structure is obtained, as shown in Fig. 5. The reflecting area can be assumed to change very slightly during this period, since the radar scans a very small fraction of the total observed volume. Even when observations are made over several hours, as shown by the three echoes, little basic variation in the type of radar echo is seen. The echoes correspond to the Hyginus area, which is one of the proposed landing sites for the Apollo mission, and the relatively sharp rise time indicates a rather smooth area. However, some small surface structure is indicated in the early part of the echo, and larger mountain structures are shown by the variations after the initial rise. One should particularly notice the large negative slope after the peak is reached, which indicates the nonuniform distribution discussed previously. As the traverse velocity increases near transit, this effect is reduced.

Figure 6 is a photograph of the Hyginus area, and even though not clearly visible, there are considerable height variations near the craters Triesnecker and Agrippa and the Ukert mountain range. These variations are more clearly seen in the impulse response of this area (Fig. 7), which is obtained by differentiating the radar return. In the differentiation, the negative slopes of the return have been set equal to zero in order to simulate the expected uniform surface structure of a fluid surface. The resultant impulse response indicates that the reflecting areas are distributed over a few hundred meters in height.

To summarize the various radar echoes that can be obtained, Fig. 8 shows echoes associated with the five different types of surface structure to be discussed, starting with the smoothest areas at the top. The increase in rise time with increasing surface structure height is apparent. The corresponding impulse responses, given in Fig. 9, show the distribution of the reflected power as the structure becomes more complex.

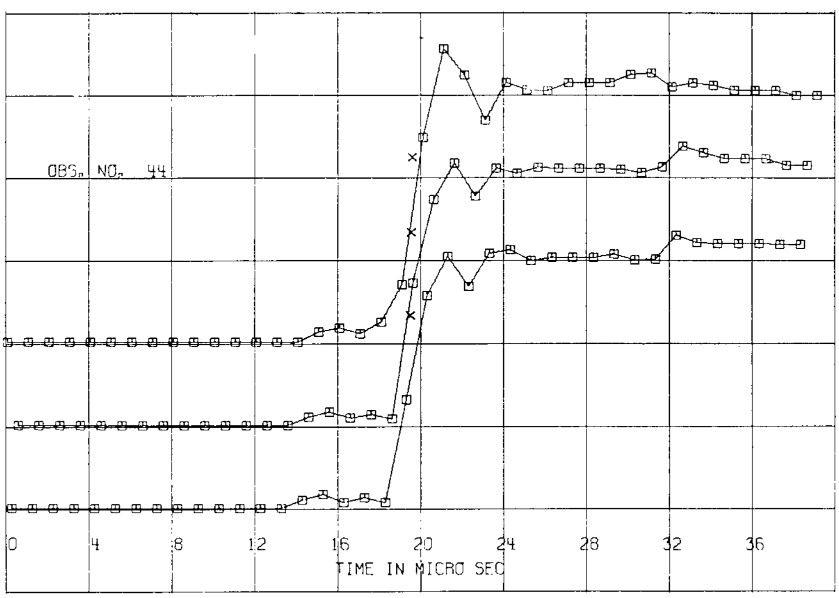

Fig. 5 - Average radar echoes of the Hyginus area obtained from 300 samples. The three curves represent data that are separated by several hours.

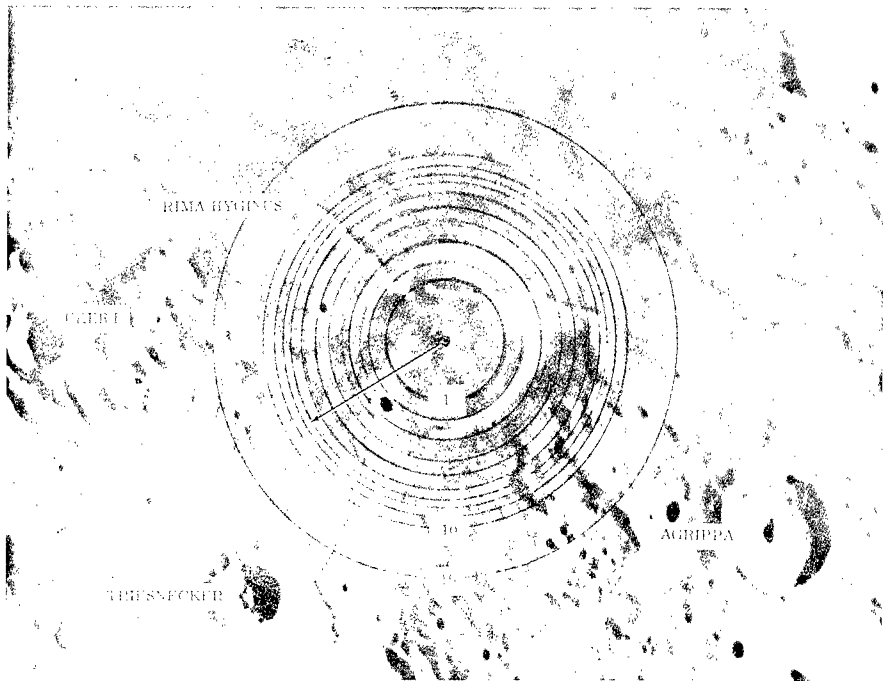

Fig. 6 - Considerable height variations are evident on the periphery of the relatively smooth Hyginus area. The spatial resolution of the radar pulse is indicated by the concentric circles.

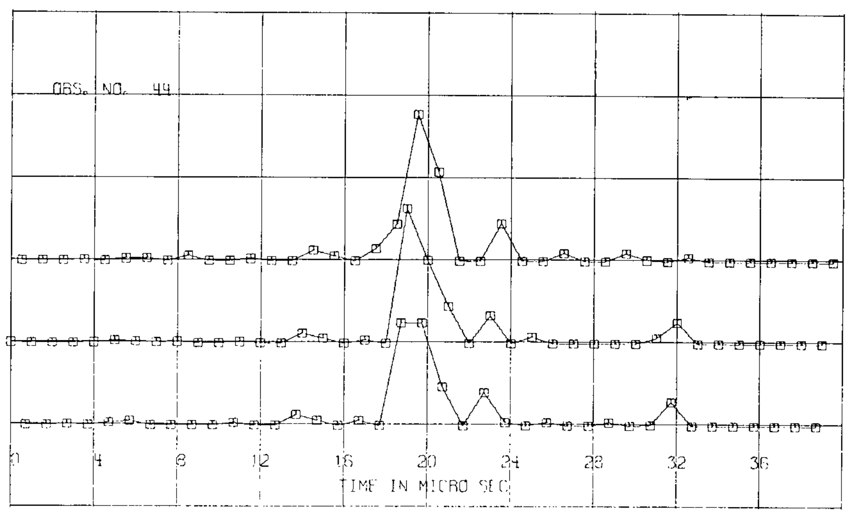

Fig. 7 - Impulse responses of the Hyginus area. These responses are obtained by differentiating the curves shown on Fig. 6.

UNCLASSIFIED

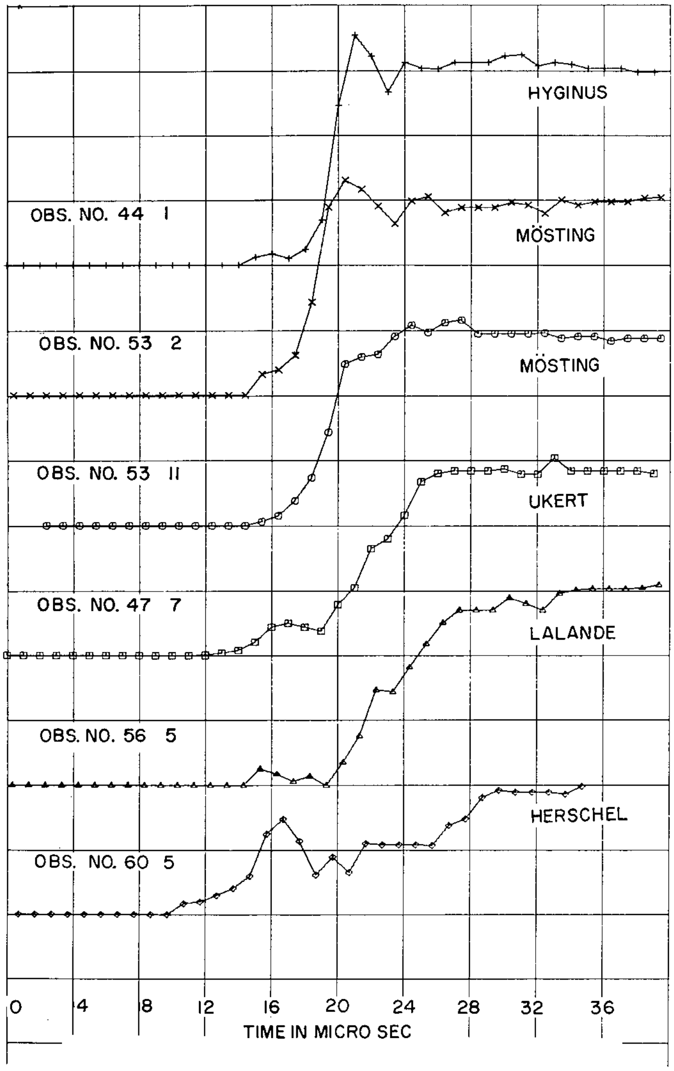

Fig. 8 - Typical radar echoes associated with the five lunar areas indicated, starting with the smoothest area (Hyginus) at the top

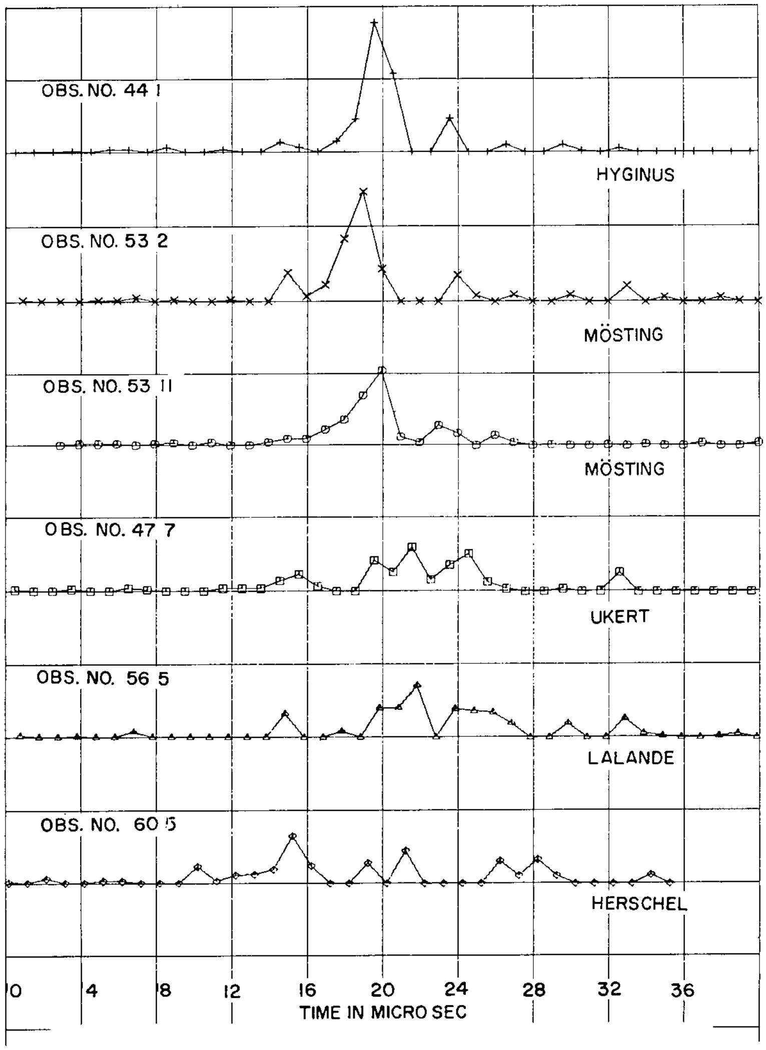

Fig. 9 - Radar impulse response for the lunar areas indicated. (See Fig. 8 for the original radar echoes.)

UNCLASSIFIED

To give some idea of the consistency, as well as the variations, of the radar echo, the radar returns over one complete day are shown for four areas (with the corresponding photographs) in Figs. 10-13. Figure 10(a) shows the Mösting area, a more complex region than Hyginus, but one that has still extensive smooth structure. This produces the still relatively short rise time shown in Fig. 10(b), but considerable variations of amplitude due to the many small Sommering mountains, as well as the larger structures near Mösting, are also present. The Hyginus area is shown again, but close to the Ukert area, in Fig. 11(a), and the corresponding radar echoes are given in Fig. 11(b). A more complex area is shown in Fig. 12(a), with the corresponding radar return in Fig. 12(b). Finally, the most complex area, near Herschel, is shown in Fig. 13(a) where the nearest reflecting area travels from a mountainous area into a more or less flat plateau imbedded in the mountain structure. In Fig. 13(b) the radar echoes near the end of the day show this change, but the gradual buildup of the rise time remains throughout the day. Finally a comparison of the radar echoes from a smooth and a rough area taken on two different days is shown in Figs. 14 and 15.

PARAMETERS DEVELOPED FROM THE DATA

The objective of the data processing was to establish simple criteria for condensing each averaged radar return to two parameters — an equivalent mean height of the observed region and the vertical size of the surface structure. The results were evaluated in terms of their internal consistency and how well they correlated with the available optical information.

UTILIZATION OF IMPULSE RESPONSE

For a true impulse response, the simplest definition of the mean height and vertical size of the surface structure would correspond to two parameters, the power centroid and the spread of the power distribution expressed as a standard deviation. This definition would be valid even if the impulse response is approximated with a finite pulse width, as long as the range resolution sufficiently exceeds the vertical size of the surface structure. If the impulse response is derived from radar returns obtained under pulse-width-limited conditions, the distribution of the surface features has to be uniform near the initial point of reflection. As has been pointed out previously, this is not fully realized for a solid surface such as the lunar surface since, in general, mountains, craters, and other surface features are not distributed uniformly and may therefore shift the centroid, as well as change the spread, of the distribution. In addition, the effect of the varying rate of motion across the observed volume during one day will modify the resulting distribution. In spite of these difficulties, some insight about the physical surface may be obtained from analyzing the pseudoimpulse response, and the results are shown for the five lunar areas in Table 1.

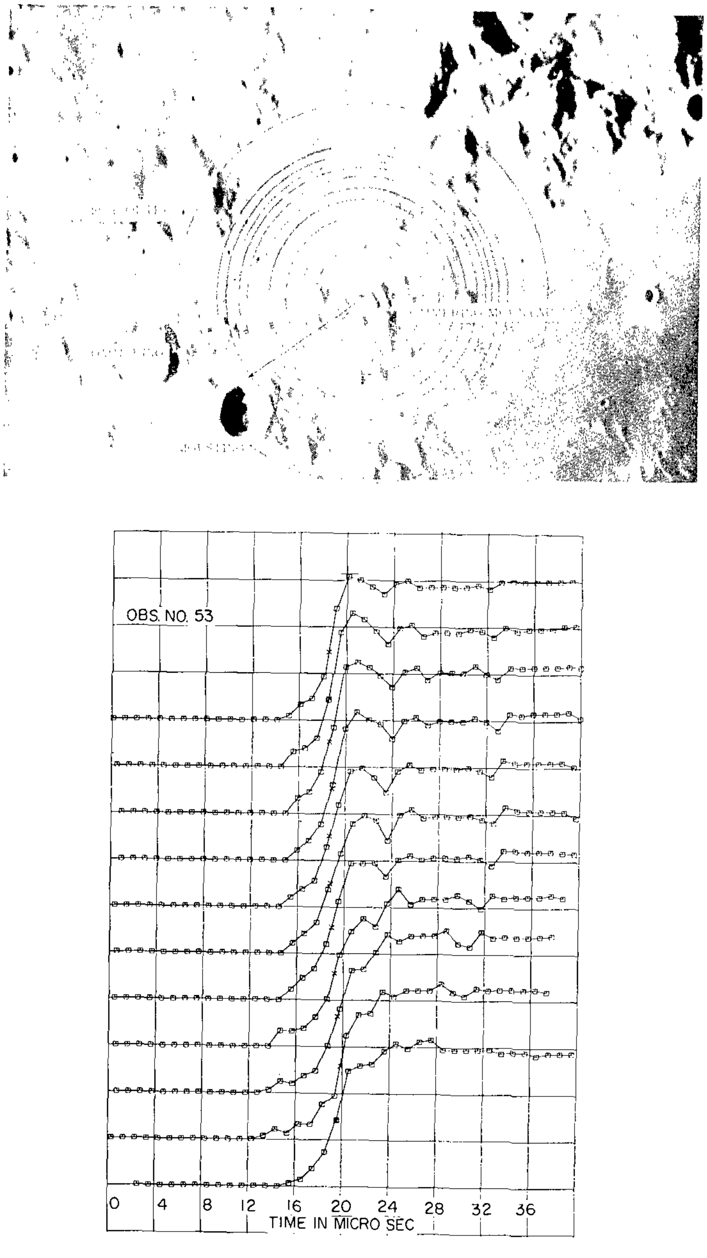

Fig. 10 - Mösting region and associated radar echoes obtained over one day

UNCLASSIFIED

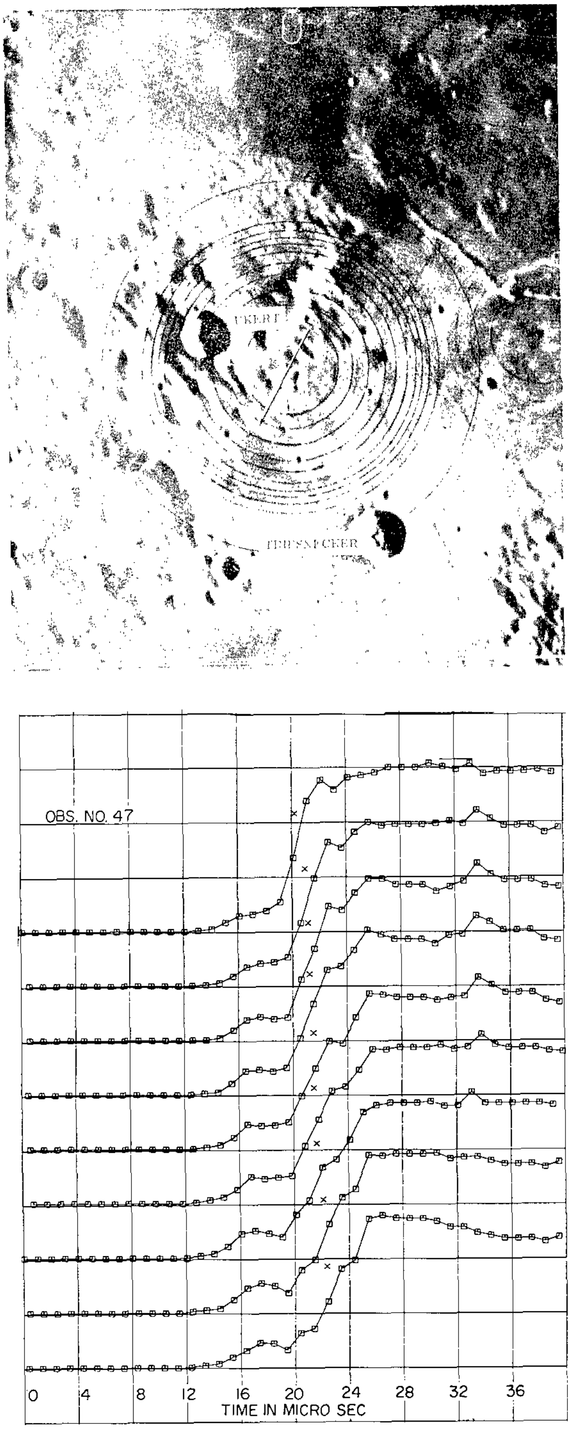

Fig. 11 - Ukert region and associated radar echoes obtained over one day

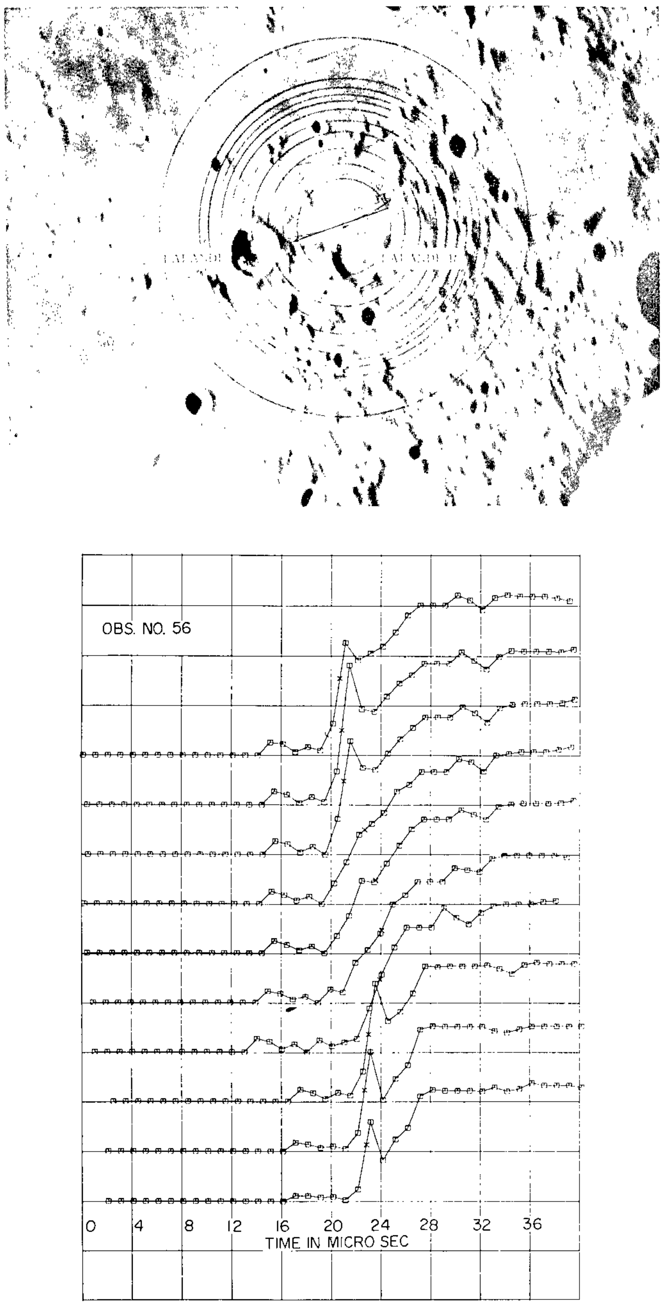

Fig. 12 - Lalande region and associated radar echoes obtained over one day. A smoothing of the initial echo rise time near transit is apparent. This is caused by the increased lunar transverse velocity near transit.

UNCLASSIFIED

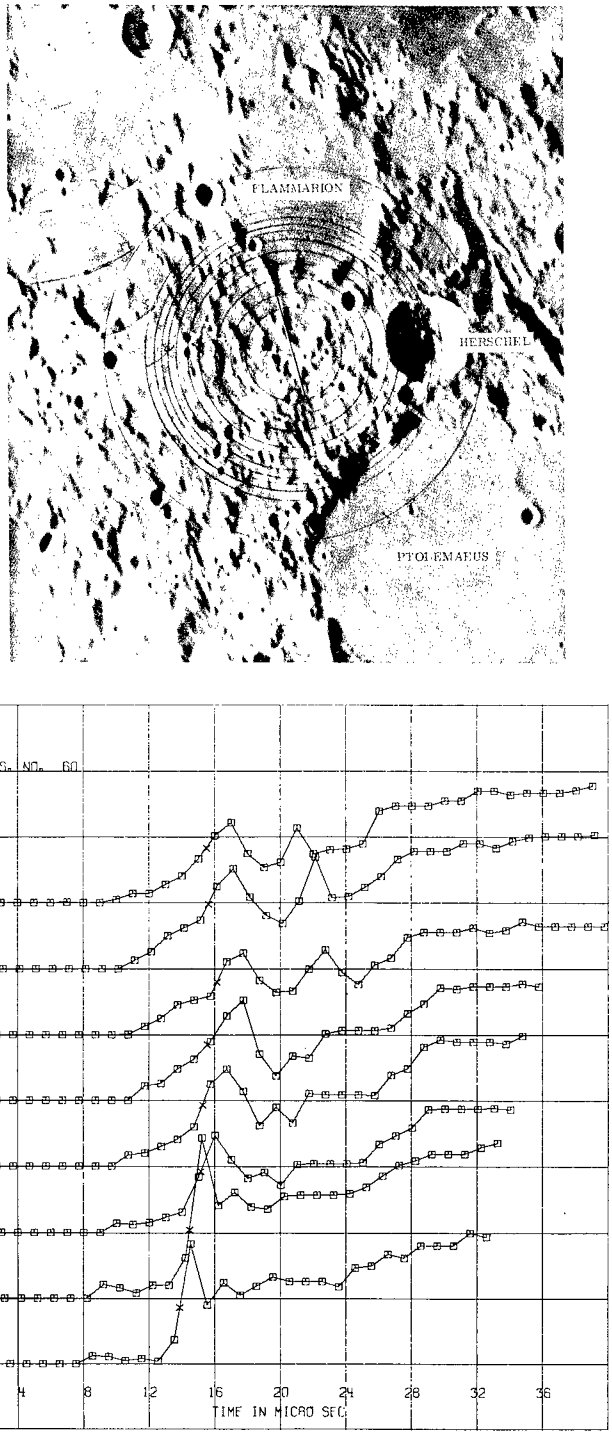

Fig. 13 - Herschel region and associated radar echoes obtained over one day

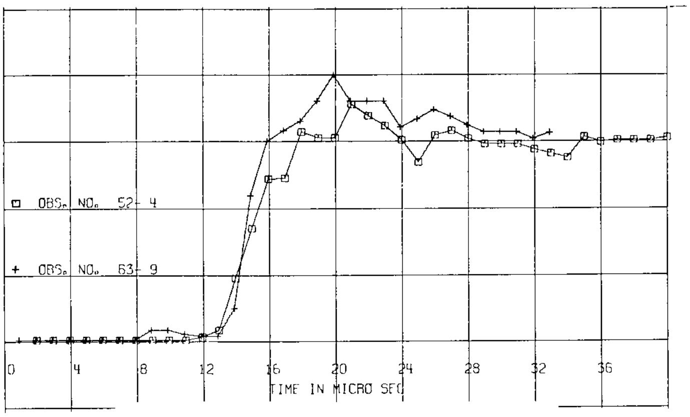

Fig. 14 - Comparison of radar echoes obtained from the same smooth lunar area on two different days

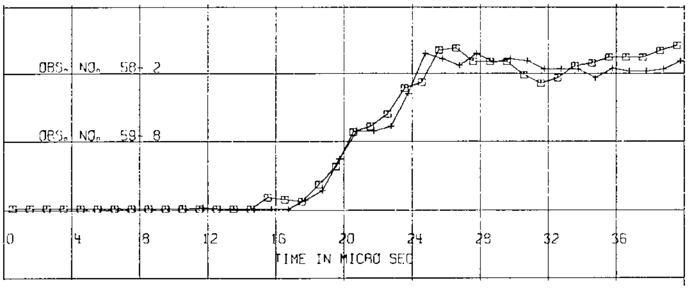

Fig. 15 - Comparison of radar echoes obtained from the same rough lunar area on two different days

The average residual centroid $\overline{\Delta t}$ and spread $\sigma_{\overline{\Delta t}}$ were obtained from the following equations:

$$\overline{\Delta t} = \frac{\sum_{i=1}^{N} a_i^2 \Delta t_i}{\sum_{i=1}^{N} a_i^2}$$

where a_i is the amplitude of the equivalent impulse response for the gate corresponding to Δt_i and the number of gates N is given by $N = 40$; and

$$\sigma_{\overline{\Delta t}} = \frac{\sum_{i=1}^{N} a_i^2 (\Delta t_i - \overline{\Delta t})^2}{\sum_{i=1}^{N} a_i^2} .$$

UNCLASSIFIED

Table 1
Average Residual Centroid $\overline{\Delta t}$ and Standard Deviation $\sigma_{\overline{\Delta t}}$ of Impulse Response Distribution for Five Lunar Areas

Obs. No.	Run No.	$\overline{\Delta t}$ (μs)	$\sigma_{\overline{\Delta t}}$ (μs)	Hour Angle (deg)	Obs. No.	Run No.	$\overline{\Delta t}$ (μs)	$\sigma_{\overline{\Delta t}}$ (μs)	Hour Angle (deg)
44	1	-3.81	0.8	-45	56	1	-3.76	2.5	-84
(Hy-	2	-3.64	1.8	-18	(La-	2	-3.86	2.1	-66
ginus)	3	-3.47	1.5	-5	lande)	3	-4.10	2.8	-45
						4	-5.55	3.8	-27
	$\overline{X}$	-3.64	1.4			5	-5.41	3.6	-7
	S	±0.17	±0.5			6	-6.01	3.5	+8
						7	-6.30	3.0	+37
53	1	-6.39	1.4	-80		8	-5.96	1.8	+57
(Mōst-	2	-6.66	2.3	-65		9	-6.07	1.9	+76
ing)	3	-6.62	2.1	-50		10	-6.33	2.1	+92
	4	-6.95	2.5	-34					
	5	-6.89	2.4	-18		$\overline{X}$	-5.34	2.7	
	6	-7.75	3.7	-3		S	+1.03	+0.7	
	7	-7.26	3.2	+15					
	8	-7.67	3.5	+37	60	1	-1.48	4.6	-90
	9	-7.76	3.0	+54	(Her-	2	-1.35	4.4	-67
	10	-7.47	1.8	+70	schel)	3	-2.26	5.3	-47
	11	-7.21	1.3	+85		4	-1.06	5.3	-20
						5	-1.03	5.5	0
	$\overline{X}$	-7.15	2.5			6	+0.22	4.9	+29
	S	±0.48	±0.8			7	+3.80	1.9	+60
						8	+2.99	2.9	+80
47	1	-2.93	1.0	-54					
(Ukert)	2	-3.98	2.3	-40		$\overline{X}$	-0.15	4.4	
	3	-4.47	3.1	-24		S	±2.00	±1.3	
	4	-5.03	3.8	-10					
	5	-5.14	3.7	0					
	6	-4.41	2.7	+14					
	7	-4.93	3.1	+32					
	8	-5.19	2.2	+46					
	9	-5.87	1.8	+51					
	$\overline{X}$	-4.66	2.6						
	S	±0.85	±0.9						

Since the observations over one day are restricted to approximately the same observed area, the results have been averaged. The following conclusions can be made:

1. The variation of the mean height and the vertical structure parameter increases with increasing surface structure.

2. Generally during any one day there is a systematic change either decreasing or increasing the mean height. Thus for a nonuniform structure, the height measurement is sensitive to the location of surface features outside the initial area.

3. The spread parameter $\sigma_{\Delta t}$ varies approximately as a cosine function of the hour angle over the day, with the maximum occurring near lunar transit. This is effectively achieved by smearing out the fine structure of the radar return due to the higher traverse speed at transit.

4. The biggest variations occur in the roughest area, both for the mean height and spread, but the percentage of variation for the spread remains approximately constant (30%).

APPLICATION TO RADAR OCEAN HEIGHT MEASUREMENTS FROM MOVING PLATFORM

The similarities between the lunar radar measurements and possible ocean satellite radar measurements have already been indicated. Both measurements employ pulse-width-limited conditions, except that the spatial resolution on the much-nearer ocean surface is determined by the curvature of the transmitted wavefront rather than by that of the observed surface. Since the vertical structure of the ocean surface is considerably smaller than the lunar surface structure, comparably narrower pulse widths will have to be employed to resolve the ocean structure. The main difference in the reflection process is that the roughness of a fluid surface will be more uniform, and this should greatly facilitate the physical interpretation of the radar return. In both cases the radar returns fluctuate due to phase interference of the reflecting facets, and while about 300 independent samples should be sufficient to obtain an averaged waveform, the time available for averaging would be reduced because of the higher velocity of the observing platform. To permit the radar to make the ocean measurements, the prime requirement appears to be sufficient radio energy to obtain a signal-to-noise ratio larger than unity for each pulse. The additional energy can be achieved by employing pulse compression, as was done for the lunar radar observations. The most significant quantity to determine initially is to measure the radar impulse response so that a description of the sea in a fundamental form is available. We are now considering how to best implement a space radar system that can provide a synoptic description of the observed ocean areas. This would require pulse widths of about 10 ns, or smaller, and some storage and computing capacity for interpreting the radar return in several range intervals.

CONCLUSIONS

The approximate shapes of impulse responses from solid rough surfaces have been shown, and the effect of the different surface structures on the energy distribution discussed. The true shape of the impulse response can be approximated from pulse-width-limited observations if the surface structure is uniformly distributed, that is, if the same topography can be assumed for the sequential annular rings on the observed surface. While this is not true generally for solid surfaces, such as the moon, it can be partially simulated by moving across the observed region during the integration interval so that the various surface features are shifted sequentially into several range intervals. For fluid surfaces, where uniform surface height variations can be assumed, a more valid representation of the impulse response should be achieved. Finally, the results of the data processing seem to indicate that for solid surfaces under pulse-width-limited conditions, the impulse response is sensitive to the location and height variations of the surface features. A more realistic impulse response of solid surfaces could be obtained if beamwidth-limited conditions are employed.

UNCLASSIFIED

ACKNOWLEDGMENT

The authors wish to express their appreciation to D. L. Hammond, R. E. Morden, K. J. Craig, R. H. Hevey and A. L. Branning, who designed and developed the lunar radar system, and obtained the data, which made this report possible.

☆ U.S. GOVERNMENT PRINTING OFFICE: 1970-397-176/139

Security Classification

UNCLASSIFIED

DOCUMENT CONTROL DATA - R & D

(Security classification of title, body of abstract and indexing annotation must be entered when the overall report is classified)

1. ORIGINATING ACTIVITY *(Corporate author)* Naval Research Laboratory Washington, D.C. 20390	2a. REPORT SECURITY CLASSIFICATION Unclassified 2b. GROUP

3. REPORT TITLE

SIMULATED OCEAN RADAR IMPULSE RESPONSES FROM LUNAR RADAR MEASUREMENTS

4. DESCRIPTIVE NOTES *(Type of report and inclusive dates)*

This is an interim report on a continuing problem.

5. AUTHOR(S) *(First name, middle initial, last name)*

A. Shapiro, B.S. Yaplee, and E.A. Uliana

6. REPORT DATE	7a. TOTAL NO. OF PAGES	7b. NO. OF REFS
May 7, 1970	22	None

8a. CONTRACT OR GRANT NO. NRL Problem G01-05 b. PROJECT NO. A37-538/F48-551-702 c. d.	9a. ORIGINATOR'S REPORT NUMBER(S) NRL Report 7050 9b. OTHER REPORT NO(S) *(Any other numbers that may be assigned this report)*

10. DISTRIBUTION STATEMENT

This document has been approved for public release and sale; its distribution is unlimited.

11. SUPPLEMENTARY NOTES	12. SPONSORING MILITARY ACTIVITY Department of the Navy (Naval Air Systems Command, and U.S. Naval Oceanographic Office), Washington, D.C. 20390

13. ABSTRACT

Measurements of the radar impulse response from rough surfaces should provide criteria for relating the radar return with the vertical structure of these surfaces. Such information is needed to utilize more efficiently ocean satellite radar observations for describing sea surface structure. While no direct measurements of the radar impulse response are available from a fluid surface, the NRL lunar high-range-resolution radar observations can provide equivalent radar impulse response measurements from a solid rough surface. The lunar radar measurements were used to simulate the ocean impulse response, and thus provide some insight into the effect of different surface roughnesses on the radar return.

The radar returns from five lunar areas of different surface roughness were analyzed and the impulse response derived. The results indicate that the size of the vertical structure correlates with the width of the impulse response, and that quantitative information concerning the parameters of mean height and surface roughness can be obtained by computing the power centroid and standard deviation of the impulse response. However, due to the nonuniform distribution of the lunar surface features, the two parameters will depend on the particular location of the surface features and the scanning speed of the radar observations.

The geometry of the ocean satellite radar observations is similar to that of the lunar radar observations, and because of the more uniform distribution of the vertical surface structure of a fluid surface, it can be expected that ocean impulse response measurements would provide more consistent data on the mean height and associated water wave heights of the observed water surface.

DD FORM 1 NOV 65 1473 (PAGE 1)

S/N 0101-807-6801

Security Classification

Security Classification

14. KEY WORDS	LINK A		LINK B		LINK C	
	ROLE	WT	ROLE	WT	ROLE	WT
Lunar topography Radar echoes Signal processing Surface roughness Echo ranging Range gating Sea states Simulation						

DD FORM 1 NOV 65 1473 (BACK)
(PAGE 2)

Security Classification